BULLETIN OF THE CHEMICAL SOCIETY OF JAPAN VOL. 39 2105—2109 (1966)

The Diffusion of Gases at High Pressures. I. The Self-diffusion Coefficient of Carbon Dioxide

By Shinji TAKAHASHI and Hiroji IWASAKI

Chemical Research Institute of Non-Aqueous Solutions, Tohoku University, Katahira-cho, Sendai

(Received December 9, 1965)

The self-diffusion coefficients of carbon dioxide were measured over a pressure range from 2 to 250 atm. at 25, 50, and 75°C. The measurements of self-diffusion through a plug of porous bronze were made using the radioactive tracer technique. The products of the density and the diffusion coefficient increase slightly with the density in the region of lower density, below about 10 mol./l., for both isotherms at 50 and 75°C, but they decrease in the region of higher density. These results agree with the results obtained by O'Hern et al., but not with Enskog's dense gas theory, and not with the values calculated by the generalized chart of Slattery et al.

The diffusion coefficient of gases at high pressure is not only an interesting physical property from the standpoint of the kinetic theory of gases, but it is also an important property for the analysis of the operations and design of apparatus in the chemical industry. Enskog[1,2] made some theoretical studies of the diffusion process in developing his kinetic theory of non-uniform gases, based on the assumption of a rigid spherical molecule. Slattery et al.[3] prepared a generalized chart for the self-diffusion coefficient of gases at high densities using Enskog's theoretical relations on transport properties and experimental data on the viscosity.

There have been some recent reports[4] on the gaseous diffusion coefficient at high densities measured by the use of either the radioactive or the stable isotope-tracer technique. However, the results have not indicated a definite relation between $D\rho$ and ρ (D: diffusion coefficient, ρ: density). For example, in the case of the self-diffusion coefficient of carbon dioxide, Drickamer et al. concluded that $D\rho$ decreases in accordance with Enskog's theory until $\rho=0.067$ g./cc., whereas O'Hern et al. stated that $D\rho$ is constant independent of the density, and Becker et al. showed that $D\rho$ increases with the density. Thus, further investigation seems to be necessary in order to clarify the relation between $D\rho$ and the density in the high pressure range.

Additional measurements of the diffusion coefficient in the $^{14}CO_2$–$^{12}CO_2$ system, by a method similar to that of O'Hern et al., will be reported here. These measurements were made at pressures up to 50 atm. at 25°C, and up to 250 atm. at 50 and 75°C. The results will be compared with the values obtained by other investigators and with the values calculated by Enskog's equation and the generalized chart.

Apparatus

The diffusion cell, the major part of the apparatus, was nearly identical with that used by O'Hern et al., Mifflin et al., and Durbin et al., as is shown in Fig. 1. The principle of measurement procedure was as follows: a diffusion path, B, composed of porous metal was placed between two chambers, C and D, equal in volume. The concentration gradient of $^{14}CO_2$ was created between these two chambers through the porous plug, and the diffusion coefficient, D_{12}, in the $^{14}CO_2$–$^{12}CO_2$ system was calculated from the measurements of the change in the concentration of $^{14}CO_2$ with time.

Each chamber had a volume of 35 cc. and was connected to the diffusion path, B, which had a length of 40 mm. and a diameter of 18 mm. The diffusion path was a plug of sintered bronze powder; two types of plugs were used, one with a grain size of ϕ160—250 μ (I) and the other, with a grain size of ϕ60—70 μ (II). The concentration of $^{14}CO_2$ was measured by means of the ionization current in the chamber. The collecting electrode, I ($20\phi\times15$ mm.), was made of invar

1) S. Chapman and T. G. Cowling, "The Mathematical Theory of Non-Uniform Gases," Cambridge University Press, London (1939).
2) J. O. Hirschfelder, C. F. Curtiss and R. B. Bird, "Molecular Theory of Gases and Liquids," John Wiley & Sons, Inc., New York (1954).
3) J. Slattery and R. B. Bird, *A. I. Ch. E. Journal*, **4**, 137 (1958).
4) K. D. Timmerhaus and H. G. Drickamer, *J. Chem. Phys.*, **19**, 1242 (1951); W. L. Robb and H. G. Drickamer, ibid., **19**, 1504 (1951); K. D. Timmerhaus and H. G. Drickamer, ibid., **20**, 981 (1952); Q. R. Jeffries and H. G. Drickamer, ibid., **21**, 1358 (1953), ibid., **22**, 436 (1954); H. A. O'Hern and J. J. Martin, *Ind. Eng. Chem.*, **47**, 2081 (1955); C. Chou and J. J. Martin, ibid., **49**, 758 (1957); E. Becker, W. Vogell and F. Zigan, *Z. Naturforsch.*, **8a**, 686 (1953); T. R. Mifflin and C. O. Bennett, *J. Chem. Phys.*, **24**, 975 (1958); V. Berry and R. Koeller, *A. I. Ch. E. Journal*, **6**, 274 (1960); L. Durbin and R. Kobayashi, *J. Chem. Phys.*, **37**, 1643 (1962); H. H. Reamer and B. H. Sage, *J. Chem. Eng. Data*, **8**, 34 (1963); I. F. Golubev and A. G. Bondarenko, *Gaz. Prom.*, **8**, 46 (1963).

steel and was insulated from the stainless steel plug, F, by a surface-polished quartz disk, E ($30\phi \times 15$ mm.). The collecting electrode, the quartz disk, and the plug were cemented together by epoxy resin. The quartz disk had a 3ϕmm. hole in its center through which the lead-in wire, H, used for measuring the ionization current, projected. The lead-in wire was insulated from the steel pipe, not shown in Fig. 1, with metharylate resin insulators and was connected to a dynamic condenser electrometer manufactured by the Okura Electric K. K. The applied voltage was maintained at about 540 V., using 12 layer-built dry cells of 45 V. each. The quantity of $^{14}CO_2$ used for each measurement was in the range of 0.01—1 μCi, and the ionization current was in the range of 10^{-13}—10^{-11} amp. The results of a preliminary experiment* are shown in Fig. 2 and Fig. 3. As is apparent in these figures, a linear relationship exists between the amount of $^{14}CO_2$ and the ionization current under these experimental conditions. The ionization currents in each of the two chambers were measured by two electrometers, and the readings were recorded during the experiment.

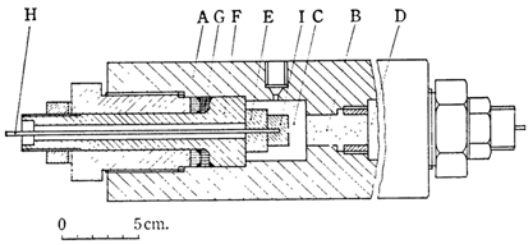

Fig. 1. Diffusion cell.

A: body, B: diffusion path, C and D: ionization chamber, E: quartz disk, F: stainless steel plug, G: teflon packing, H: lead-in wire, I: collecting electrode.

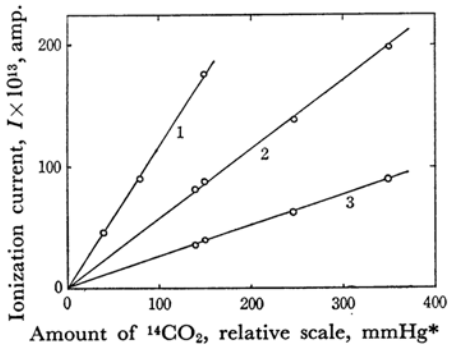

Fig. 2. Relations between the amount of $^{14}CO_2$ and ionization current at 25°C.
1: 8 atm., 2: 20 atm., 3: 50 atm.

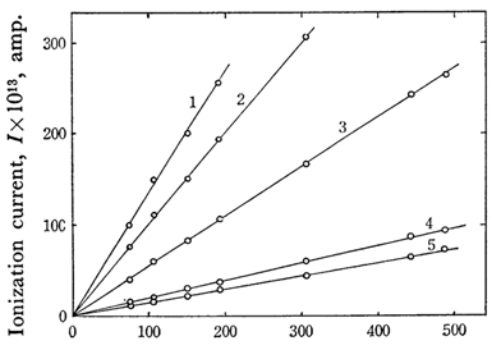

Fig. 3. Relations between the amount of $^{14}CO_2$ and ionization current at 50°C.
1: 10 atm., 2: 20 atm., 3: 50 atm., 4: 100 atm., 5: 200 atm.

An air thermostat was used. The temperature was kept within ±0.1°C by a combination of a platinum resistance thermometer, a Wheatstone bridge, and a photoelectric cell circuit,[5] and was measured by a platinum resistance thermometer calibrated against the freezing and boiling points of water and a PTR thermometer. The pressure was measured by a Bourdon gauge calibrated against a pressure balance of a free-piston type. The errors in pressure measurements were within ±0.02 atm. up to 20 atm., ±0.1 atm. in the 10—50 atm. range, and ±0.5 atm. in the 50—250 atm. range.

The radioactive $^{14}CO_2$ was generated by adding 60% $HClO_4$ to $Ba^{14}CO_3$; its specific radioactivity was approximately 1 μCi/cc. at N.T.P. The non-radioactive carbon dioxide, with a purity of over 99.9% and with a water content of less than 0.04%, was used after it had been dried over phosphorus pentoxide.

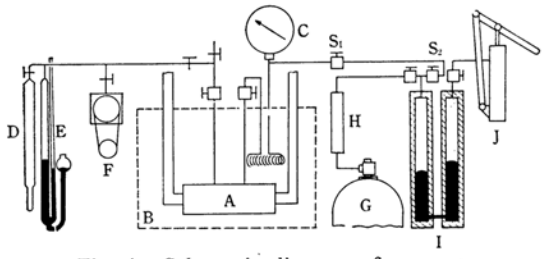

Fig. 4. Schematic diagram of apparatus.

A: diffusion cell, B: air thermostat, C: pressure gauge, D: $^{14}CO_2$ container, E: gas burette, F: vacuum pump, G: $^{12}CO_2$ cylinder, H: drying tube, I: intensifier, J: oil pump, S_1 and S_2: valves

* The experimental procedures were as follows: after the ionization chamber had been evacuated, a mixture of $^{14}CO_2$ and $^{12}CO_2$ was introduced into the chamber (70—500 mmHg). These pressures are shown as abscissae in Fig. 2 and Fig. 3. The amounts of $^{14}CO_2$ are proportional to these pressures. Then, the pressure of the chamber was raised to 10—200 atm. by introducing $^{12}CO_2$, and the ionization current was measured.

5) K. Date, G. Kobuya and H. Iwasaki, *Bulletin of The Chemical Research Institute of Non-Aqueous Solutions, Tohoku Univ.*, **10**, 67 (1961).

Experimental

The arrangement of the experimental apparatus is shown in Fig. 4. An air thermostat was adjusted to a pre-determined temperature and allowed to stand for approximately 24 hr. Cell A was then evacuated to approximately 10^{-2} mmHg by a vacuum pump, F. A suitable quantity of $^{14}CO_2$ was introduced through the gas burette, E, from the $^{14}CO_2$ container, D, into the left chamber in the cell. The non-radioactive carbon dioxide was introduced into the right chamber from the cylinder, G, through the drying tube, H, and compressed to a given pre-determined pressure by the oil pump, J. In this way a major portion of the $^{14}CO_2$ was collected in the left chamber and a large concentration gradient of $^{14}CO_2$ was created between the two chambers through the porous plug. Then, the diffusion cell was disconnected from the pressure system between the two valves, S_1 and S_2, and the voltage was applied to cell, A; the resulting ionization current was measured and recorded. An example is shown in Fig. 5.

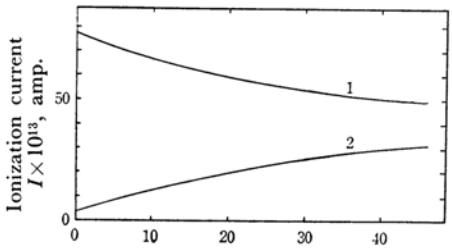

Fig. 5. The variation of ionization current with time at 50°C, 84.2 atm.
1: I_1, 2: I_2

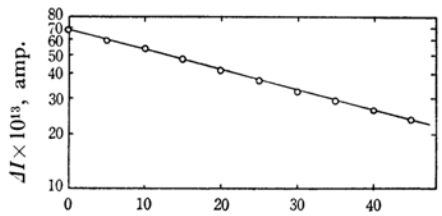

Fig. 6. Semilog plot of current difference ΔI vs. time at 50°C, 84.2 atm.

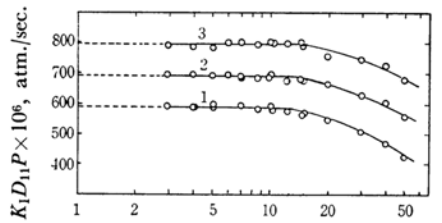

Fig. 7. Relations between $K_I D_{11} P$ and P.
1: 25°C, 2: 50°C, 3: 75°C

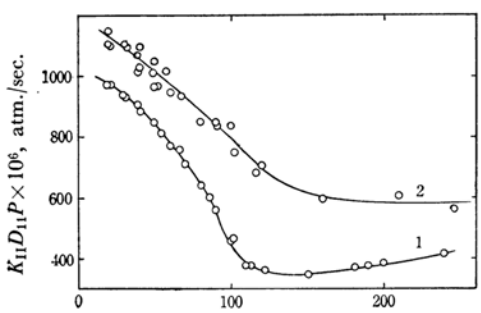

Fig. 8. Relations between $K_{II} D_{11} P$ and P.
1: 50°C, 2: 75°C

Calculation

Assuming that the concentration gradient of $^{14}CO_2$ in the diffusion path is linear and that the concentration in each chamber is uniform, the following equations are obtained:

$$\ln(C_1 - C_2) = -KD_{12}t + \text{constant} \tag{1}$$

$$K = \frac{A}{L}\left(\frac{1}{V_1} + \frac{1}{V_2}\right) \tag{2}$$

where C_1 and C_2 are concentrations of $^{14}CO_2$ in chamber 1 and chamber 2, shown as C and D, respectively in Fig. 1, where D_{12} is the mutual diffusion coefficient in the $^{14}CO_2$-$^{12}CO_2$ system, and where t is the time. K is an apparatus constant; it is given by Eq. 2, where A and L are the effective cross section and the effective length of the diffusion path and where V_1 and V_2 are the volumes of chamber 1 and chamber 2 respectively. Since a linear relationship holds between the concentration of $^{14}CO_2$ and the ionization current, Eq. 1 may be written as:

$$\ln \Delta I = -KD_{12}t + \text{constant} \tag{3}$$

$$\Delta I = I_1 - \gamma I_2$$

$$\gamma = I_1'/I_2'$$

where I_1 and I_2 are the ionization currents in chamber 1 and chamber 2 respectively. I_1' and I_2' are the ionization currents in chamber 1 and chamber 2 respectively, when $^{14}CO_2$ is introduced into the chambers at the same concentration. According to Eq. 3, ln ΔI should be linear with t; this was experimentally proved, as is shown in Fig. 6, where common logarithms are used. If ΔI at time t_i and t_f are designated as $(\Delta I)_i$ and $(\Delta I)_f$ respectively, KD_{12} can be calculated by the following equation:

$$KD_{12} = \frac{6.3961\times10^{-4}}{\Delta t}\log\frac{(\Delta I)_i}{(\Delta I)_f} \tag{4}$$

where the terms are expressed as follows: K; 1/cm², D_{12}; cm²/sec., Δt; hr., and ΔI: amp. Hutchinson[6]

6) F. Hutchinson, *J. Chem. Phys.*, **17**, 1081 (1949).

verified the following relationship between the self-diffusion coefficient, D_{11}, and the mutual diffusion coefficient, D_{12} at normal pressure:

$$\frac{D_{11}}{D_{12}}=\left[\left(\frac{m_1m_2}{m_1+m_2}\right)\left(\frac{m_1+m_1}{m_1m_1}\right)\right]^{1/2}=\left(\frac{2m_2}{m_1+m_2}\right)^{1/2} \quad (5)$$

where m_1 and m_2 are masses of gaseous molecular species containing isotopes. Assuming that the above relationship also holds in the high pressure region, the D_{11} value in the $^{12}CO_2$ system was obtained by multiplying the D_{12} measured in this work by 1.011.

Results

When Diffusion Path I was Used.—In the 2—50 atm. pressure range, a type-I porous plug was used as the diffusion path. The values of $K_ID_{11}P$ obtained are shown in Fig. 7. The values of K_ID_{11} at 1 atm. were then obtained by extrapolation using the observed values of $K_ID_{11}P$. The apparatus constant, K_I was determined by the use of the values of D_{11} reported by Amdur et al.[7] at 1 atm. These are shown in Table I. The values of D_{11} calculated using K_I, which is given in Table I, are shown in Table II. The smoothed values of D_{11} obtained from the values in Table II are shown in Table III. The deviation of the

TABLE I. DETERMINATION OF APPARATUS CONSTANT K_I

Temp. °C	P atm.	$K_ID_{11}P\times10^6$ atm./sec.	$D_{11}\times10^3$* cm²/sec.	$K_I\times10^3$ 1/cm²
25	1.0	591	114.0	5.19
50	1.0	689	132.7	5.20
75	1.0	795	152.3	5.22

* Measured by Amdur et al.[7]

TABLE II. EXPERIMENTAL RESULTS FOR DIFFUSION PATH I

25°C		50°C		75°C	
P atm.	$D_{11}\times10^3$ cm²/sec.	P atm.	$D_{11}\times10^3$ cm²/sec.	P atm.	$D_{11}\times10^3$ cm²/sec.
2.91	39.1	2.91	45.8	2.91	52.1
2.91	39.2	3.91	34.2	3.91	38.7
3.91	29.0	4.91	26.9	4.91	30.7
3.91	28.7	5.89	22.7	5.89	26.1
4.91	23.5	6.81	19.4	6.87	22.4
4.91	23.2	6.87	19.1	8.74	17.4
6.81	16.7	8.74	15.0	10.68	14.4
8.74	12.8	10.3	12.8	11.4	13.5
10.30	11.0	10.68	12.5	12.61	12.1
10.68	10.4	12.61	10.3	14.55	10.6
12.61	8.78	14.55	8.98	15.3	9.81
14.55	7.43	15.3	8.50	20.5	7.09
15.3	7.15	20.5	6.21	30.4	4.71
20.5	5.12	30.4	3.98	40.4	3.45
30.4	3.20	40.4	2.88	50.5	2.59
40.4	2.23	50.4	2.13		
50.4	1.61				

TABLE III. SMOOTHED VALUE OF $D_{11}\times10^3$, cm²/sec.

P, atm.	25°C	50°C	75°C
10.0	11.2	13.2	15.2
20.0	5.30	6.35	7.48
30.0	3.26	4.05	4.81
40.0	2.25	2.90	3.51
50.0	1.62	2.18	2.71

TABLE IV. DETERMINATION OF APPARATUS CONSTANT K_{II}

Temp. °C	P atm.	$K_{II}D_{11}P\times10^6$ atm./sec.	$K_{II}\times10^3$ 1/cm²
50	20	970	7.64
50	30	930	7.65
50	40	880	7.59
50	50	830	7.61
		Average	7.62
75	20	1130	7.55
75	30	1090	7.57
75	40	1050	7.49
75	50	1005	7.42
		Average	7.51

TABLE V. EXPERIMENTAL RESULTS FOR DIFFUSION PATH II

50°C		75°C	
P atm.	$D_{11}\times10^3$ cm²/sec.	P atm.	$D_{11}\times10^3$ cm²/sec.
19.2	6.62	20.2	7.20
22.4	5.69	20.3	7.22
29.9	4.11	21.1	7.24
30.3	4.00	30.3	4.84
40.0	2.95	32.3	4.52
40.8	2.83	40.1	3.40
49.8	2.21	40.1	3.54
53.1	1.99	40.4	3.33
58.8	1.70	41.2	3.54
67.1	1.47	50.1	2.77
70.9	1.31	50.2	2.67
80.7	1.03	50.2	2.54
86.7	0.907	50.5	2.49
92.5	0.792	58.1	2.33
98.0	0.678	61.0	2.06
101.7	0.600	67.4	1.85
102.2	0.595	81.5	1.42
109.5	0.453	91.5	1.23
113.2	0.436	92.5	1.20
123.3	0.379	99.4	1.12
150.3	0.297	103.5	0.956
182.5	0.266	117.5	0.770
189.4	0.260	123.1	0.759
199.4	0.250	158.5	0.503
240.0	0.228	208.3	0.386
		245.6	0.303

7) I. Amdur, J. W. Irvine, Jr., E. A. Mason and J. Ross, *J. Chem. Phys.*, **20**, 436 (1952).

experimental value from the smoothed value reaches a maximum of 3.6%; on the average it is 0.9%.

When Diffusion Path II was Used.—When the type-I porous plug was used for the measurements at pressures over 100 atm., the plot of $\log \Delta I$ against t presented a convex curve downwards; thus, the assumption made for the derivation of Eq. 1 became invalid. However, a type-II porous plug gave no such trouble during experiments at higher pressures.

The values of $K_{II}D_{11}P$ obtained at 50 and 75°C and in the range of 20—250 atm. are shown in Fig. 8. From the smooth curves, the smoothed values of $K_{II}D_{11}P$ at 20, 30, 40, and 50 atm. were obtained; they are shown in the third column of Table IV. By using the smoothed values of D_{11} at 20—50 atm. shown in Table III, K_{II} was calculated; it is shown in the last column of Table IV. The values of D_{11} calculated using these K_{II} values are shown in Table V.

Discussion

From the standpoint of the kinetic theory of gases, Enskog[1,2] derived the following equations for the diffusion coefficient of gases at high pressures, assuming a rigid sphere as the molecular model:

$$D = (D_{11})^\circ/\chi \tag{6}$$

$$(D_{11})^\circ = \frac{3}{8}\sqrt{\frac{\boldsymbol{k}T}{\pi m}}\frac{1}{n\sigma^2\Omega^{(1,1)*}} \tag{7}$$

$$\chi = 1 + 0.625\left(\frac{2}{3}\pi n\sigma^3\right) + 0.2569\left(\frac{2}{3}\pi n\sigma^3\right)^2 + 0.115\left(\frac{2}{3}\pi n\sigma^3\right)^3 + \cdots \tag{8}$$

where $(D_{11})^\circ$ is a value which can be calculated from the relationship applicable at the normal pressure and which is approximately given by Eq. 7, where χ is the correction factor due to the pressure rise and is given by Eq. 8, where $\boldsymbol{k}$ is Boltzmann's constant, where m is the mass of the molecule, where n is the number of molecules in a unit volume, where $\Omega^{(1,1)*}$ is the reduced collision integral, and where σ is a constant related to the intermolecular potential. It can be seen from Eq. 7 that $(D_{11})^\circ$ is a function of the temperature alone in the vicinity of the normal pressure. By Enskog's theoretical equation (6), $D_{11}\rho = (D_{11})^\circ\rho/\chi$ and $D_{11}\rho$ is dependent not only on the temperature, but also on χ, that is, on ρ. Therefore, it is convenient to study the relationship between $D_{11}\rho$ and ρ.

In Fig. 9, $D_{11}\rho$ is plotted against ρ. The values of ρ were calculated by using the compressibility data of Michels et al.[8] The plot shows a close similarity to that of the results obtained by O'Hern et al. The values at 35°C, which were interpolated from our experimental values, were always higher than their experimental values, but the differences were never more than 5%. On the other hand, there were large deviations in the experimental values of Drickamer et al., and so their values could not be used for an accurate comparison. The relative values of $D_{11}\rho$, obtained by Becker et al., were expressed as 1.00 at 20°C and 15 atm., 1.08 at 40 atm., and 1.26 at 50 atm., and they showed a rapid increase with the pressure, thus indicating an entirely different tendency from the results obtained by the present authors.

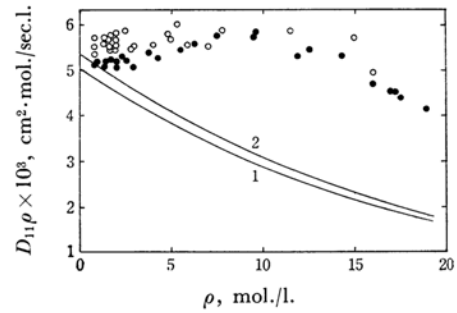

Fig. 9. Comparison of the measured values with the values calculated by Enskog's theory.
Experimental: ●—50°C, ○—75°C
Theoretical: 1—50°C, 2—75°C

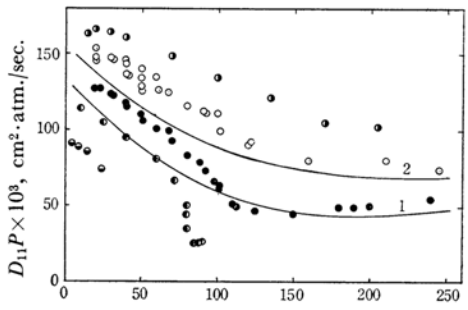

Fig. 10. Comparison of the measured values with the values calculated by the generalized chart.
Present work: ●—50°C, ○—75°C
O'Hern et al.: ◑—100°C, ◐—35°C, ◒—0°C
Calculated: 1—50°C, 2—75°C

The values calculated by substituting $\sigma = 3.996$ Å in Eq. 8 are shown as solid lines in Fig. 9. The deviations increase with the pressure, amounting to approximately 50% when $\rho = 10$ mol./l. Even if the decrease in σ with the pressure was taken into account in Eq. 8, in accordance with the consideration of O'Hern et al., a theoretical relation which fits the experimental values could not be obtained.

The values of $D_{11}P$ calculated from the generalized chart are shown as solid lines in Fig. 10. The deviation from our experimental values is approximately 20% in the vicinity of 50 atm., but it decreases over 100 atm.

8) A. Michels and C. Michels, *Proc. Royal Soc.*, **A153**, 201 (1936); **A160**, 348 (1937).